ELSEVIER

Journal of Hydrology 216 (1999) 99–110

Journal of Hydrology

Evaluation of an empirical equation for annual evaporation using field observations and results from a biophysical model

Bhaskar J. Choudhury

Hydrological Sciences Branch (Code 974), Laboratory for Hydrospheric Processes, NASA Goddard Space Flight Center, Greenbelt, MD 20771, USA

Received 22 April 1998; received in revised form 23 October 1998; accepted 26 November 1998

Abstract

An empirical equation for annual evaporation (E) of the form, $E = P/\{1 + (P/R_n)^{\alpha}\}^{1/\alpha}$, where P is the annual precipitation, R_n the water equivalent of annual net radiation, and α an adjustable parameter, is evaluated using field observations (water balance, and micrometeorologic measurements for areas ca. 1 km^2) at eight locations having different types of vegetation, and results from a biophysical process-based model for four years (1987–1990) for ten river basins (areas larger than 10^6 km^2). For the field observations, minimum value of the mean absolute error (MAE) was 33 mm (4% of the mean observed evaporation) obtained for $\alpha = 2.6$, and the empirical equation was able to explain 99% of the variance under linear least square regression, with a slope of 0.99, intercept of 16 mm, and standard error of estimate (SEE) of 46 mm. For evaporation from the river basins, minimum value of the MAE was 36 mm (5% of the mean evaporation) obtained for $\alpha = 1.8$, and the empirical equation was able to explain 97% of the variance, with linear regression slope of 1.01, intercept of -11 mm, and SEE of 45 mm. The effect of spatial variations in P and R_n in determining evaporation from the empirical equation is analyzed to develop an understanding of the differences in the value of α for the field observations and the river basins.

Keywords: Evaporation; Modeling; Spatial variation

1. Introduction

A knowledge of evaporation at varied spatial and temporal scales is needed in hydrologic, meteorologic and ecologic studies, and a range of modeling and measurement procedures have been developed to determine evaporation at these scales (Lieth, 1975; Brutsaert, 1982; Foley et al., 1996). Empirical equations relating annual evaporation or runoff to precipitation have been developed for global water balance calculations because of inadequate runoff data for many parts of the world and for extrapolating runoff from the last gauging station to the mouth of large river basins (Korzun, 1978, pp. 141–145; L'vovich, 1979, pp. 75–102).

While calculating the climatologic global evaporation, Budyko (1958, pp. 144–145) found that the following equation for annual evaporation (E), derived as the geometric mean of empirical equations proposed by Schreiber (1904) (the first bracketed term in Eq. (1)) and Ol'dekop (1911, p.154) (the second bracketed term in Eq. (1)),

$$E = [\{P(1 - \exp(-E_0/P))\}\{E_0 \tanh(P/E_0)\}]^{0.5}, \quad (1)$$

where E_0 is the annual potential evaporation (maximum possible evaporation) and P the annual precipitation, gave more accurate results than either of the component equations for 29 European river basins larger than 10 000 km^2. Budyko (1958, pp. 157–159,

0022-1694/99/$ - see front matter
PII: S0022-1694(98)00293-5

162–164, 174) calculated E_0 from energy balance equation or equated it to water equivalent of net radiation for a moist surface which was defined as a surface whose albedo is 0.18 (during the warm season) and surface temperature is equal to air temperature. However, Schreiber considered E_0 to be an adjustable parameter, while Ol'dekop (1911, p.154–160) calculated E_0 (mm) for the summer six months' (May–October) total as 102 D and for the winter six months' total as 72*D*, where *D* is the vapor pressure deficit (hPa) of air (the basis for this method is not clearly documented). By modifying Budko's calculation of E_0, Packer and Sangal (1971) found that runoff (Q) calculated using Eq. (1) ($Q = P - E$) was within 5% of the measured values for 31 catchments with areas 181– 9091 km^2 in Southern Ontario.

In contrast to Eq. (1), which was assessed using long-term average values of P and Q, Pike (1964) found the following equation:

$$E = P/\{1 + (P/E_0)^2\}^{0.5}, \tag{2}$$

could explain *interannual variations* of evaporation within 10% for four catchments with areas 790–2330 km^2 within Malawi when E_0 was calculated from either Penman's (1948) equation or by adjusting pan measurements. Similar to Eq. (1), the limits of evaporation in Eq. (2) are given by P and E_0, although the method for calculating E_0 is not identical. Pike (1964) had proposed Eq. (2) as a modification of a similar equation previously found by Turc (1954) based on 254 catchments of areas ca. 5–626 000 km^2 from four continents (Africa, Asia, Europe, and North America), who had calculated E_0 as $(300 + 25T + 0.05T^3)$, where T is the mean annual air temperature (°C).

Although functional forms of Eqs. (1) and (2) are different, numerical values predicted by these two equations do not differ greatly (ca. 3%) when same values of P and E_0 are used (Dooge, 1992). However, as noted earlier, varied methods were used to calculate E_0, and these methods can give substantially different results (Budyko, 1958, pp. 161–174); Bovis and Barry, 1974; Zubenok, 1976, Tables 27–29; Liang, 1982). Further, as E depends non-linearly on P and E_0, one would expect these equations to be affected by spatial scale or variabilities in P and E_0 (as elaborated later, areally averaged values of P and E_0 in these equations may not provide areally averaged E). Thus, recognizing that the catchments considered by Turc (1954), Budyko (1958) and Pike (1964) had vastly different areas, the following question arises: are these equations independent of spatial scale?

Considering that precipitation and net radiation are fundamental, measurable fluxes appearing in water and energy balance equations, and Pike's success in explaining interannual variation of evaporation, the objective of this study is to assess to what extent a generalized form of Eq. (2), viz.,

$$E = P/\{1 + (P/R_n)^\alpha\}^{1/\alpha}, \tag{3}$$

where R_n is the water equivalent of annual net radiation and α an adjustable parameter, can explain annual evaporation. Our hypothesis is that α will change from spatial scales of micrometeorologic measurements (areas ca. 1 km^2) to large river basins (areas ca. 10^6 km^2) because of the likely differences in spatial variations in P and R_n at these scales.

Eq. (3) assumes that the annual evaporation will not exceed corresponding to P or R_n. Unlike Eqs. (1) and (2), Eq. (3) acknowledges that evaporation from different types of vegetation could be different owing to associated net radiation (i.e., albedo and surface temperature), although physiologic and aerodynamic control on evaporation are not recognized.

Eq. (3) defines a family of curves as the value of α changes. Some general characteristics of these curves can be illustrated analytically, as follows:

For small values of μ ($= P/R_n$), which will occur in hot and temperature deserts, E varies as:

$$E = P[1 - (1/\alpha)\mu^\alpha]. \tag{4}$$

It follows from Eq. (4) that the parameter α needs to be greater than 0 if the runoff coefficient $Q/P\{ = 1 - (E/P)\}$ is to approach zero as P approahces zero. Also, departure of E from P will decrease as α increases.

Similarly, for large values of μ, which can occur in tropical humid and tundra areas, E varies as:

$$E = R_n[1 - (1/\alpha)\mu^{-\alpha}], \tag{5}$$

which shows that departure of E from R_n will decrease as α increases.

Eq. (3) represents a curve of two intersecting lines, $E = P$ (when $P < R_n$) and $E = R_n$ (when $P > R_n$), as α tends to infinity. By the Taylor series expansion,

Table 1
Field data for annual precipitation (P), water equivalent of net radiation (R_n), and evaporation (E) in millimeters used to evaluate the empirical equation. Location name, its coordinate (latitude and longitude in integer degrees, with positive values for north and east), vegetation type, and source are given. Data for a specific 12 month period and average of many years are noted as, respectively, 1 and LT, together with the method used to determine evaporation are given in the Comment

Location	Coordinate	Vegetation	P	R_n	E	Source	Comment
Manaus[a]	−3, −60	Rainforest	2801	1424	1344	Shuttleworth, (1988)	1, Micrometeorologic
Manaus[b]	−3, −60	Rainforest	2539	1502	1288	Shuttleworth, (1988)	1, Micrometeorologic
Tucson	32, −111	Desert	275	1180	262	Unland et al., (1996)	1, Micrometeorologic
Agarape Acu	−1, −48	Trop.secondary	1819	1772[c]	1363	Holscher et al., (1997)	1, Micrometeorologic
Cabauw	52, 5	Grass	926[d]	520	523	Beljaars and Bosveld, (1997)	1, Micrometeorologic
Hartheim	48, 8	Pine	731	985	610	Jaeger and Kessler, (1997), Vogt and Jaeger, (1990)	1, Micrometeorologic
Hartheim	48, 8	Pine	645	1085	622	Jaeger and Kessler, (1997)	LT, Water balance
Janlappa	−7, 106	Rainforest	2851	1543	1481	Calder et al., (1986)	1, Water balance
Parsons	39, −79	Oaks/Maple	1455	890	817	Tajchman et al., (1997)	LT, Water balance
Pt. Barrow	71, −157	Tundra	175	182	72	Brown et al., (1968), Maykut and Church (1973) Ryden, (1981)	LT, Water balance

[a] September 1983 – August 1984.
[b] September 1984 – August 1985.
[c] Based on monthly E and E/R_n ratio given by the authors.
[d] Adjusted for gauge undercatch caused by wind (estimated to be 17%) and evaporation loss because of gauge wetting (3%) based on data given by the authors.

one can relate evaporation for two nearby values of α, namely $E(\alpha)$ and $E(\alpha')$, as:

$$\frac{E(\alpha')}{E(\alpha)} = 1 + \frac{(\alpha' - \alpha)\{(1+\mu^{\alpha})\ln(1+\mu^{\alpha}) - \mu^{\alpha} \ln \mu^{\alpha}\}}{\alpha^2(1+\mu^{\alpha})}. \quad (6)$$

One can verify that, for given α and α', the ratio $E(\alpha')/E(\alpha)$ attains its maximum value for $\mu = 1$, and thus, an accurate knowledge of evaporation at this value of μ might provide a better distinction of α values. Also, $E(\alpha') > E(\alpha)$ when $\alpha' > \alpha$, i.e., for a given μ, E increases (decreases) as α increases (decreases).

2. Data and methods

2.1. Field observations

Field observations used to assess Eq. (3) are given in Table 1, together with sources of these data. Micrometeorologic measurements are based on eddy correlation (near Manaus and Tucson), sigma-T (near Tucson), the Bowen ratio- (near Tucson and Agarape Acu) and aerodynamic-energy balance methods (near Cabauw and Hartheim). These measurements were necessarily supplemented by modeling or interpolation to fill data gaps. The water balance method was used to determine evaporation near Hartheim, Janlappa, Parsons, and Point Barrow. Detailed description of the measurements and surface characteristics can be found in the quoted sources. Briefly, 90% of the flux measured near Manaus originated within 1.8 km of the tower, and except for a narrow range of angles, the tower had fetches of undisturbed (natural) tropical forest. Desert vegetation near Tucson consisted of shrubs and cacti (40% vegetation cover), with sparse grasses growing during spring and following summer rainfalls. The eddy correlation system was on top of a 6 m tower (80% of the flux orginated within 282 m of the tower), while the Bowen ratio sensors were at 3 and 10 m above the ground (80% of the flux originated within 67 and 544 m of the tower for the lower and upper sensors, respectively). The sigma-T systems were variously

Table 2
The mean and range of annual evaporation (mm) from river basins calculated using a biophysical process-based model for 1987–1990, together with climatologic evaporation determined by Korzun (1978) and the per cent absolute difference between the mean and Korzun's values. The area of these river basins in units of million square kilometer is also given

Basin	Area	Mean	Range	Korzun	Difference (%)
Amazon	7.0	1038	994–1085	1060	2
Changjiang	1.8	664	639–703	605	10
Congo	3.7	1034	953–1112	1070	3
Mississippi	3.3	589	498–647	641	8
Nile	3.0	523	511–543	620	16
Ob	3.0	393	367–423	400	2
Parana	3.0	951	876–1018	902	5
St. Lawrence	1.2	588	579–600	625	6
Volga	1.4	474	446–503	470	1
Yenisey	2.6	341	330–349	320	7
All Basins		660		671	2

installed at heights of 5, 7, and 10 m above the ground. Approximately 2.5-year old secondary forest under seasonal rainfall near Agarape Acu consisted of many woody species, and psychrometers were installed at 2.77 and 5.72 m above the ground, which were later raised to 3.2 and 6.7 m because of the increasing vegetation height. Grass at the Cabauw site was kept at a height of about 0.08 m by frequent mowing, and effective roughness length representative of a few kilometers surrounding the tower, wind speed at 10 m and temperature difference at 0.6 and 10 m were used to determine sensible heat flux. Aerodynamic profile measurements up to a height of ca. 30 m near Hartheim are for a stand of Scots pine covering an area of 1.5 km^2. Vegetation in the Janlappa nature reserve was secondary rainforest, although not untypical of primary forest, and water balance was done on a plot of area ca. 0.07 km^2. The water balance near Parsons is for a temperate deciduous forest consisting of varieties of oak, sugar maple, black cherry, etc. (0.4 km^2 catchment). Tundra vegetation on the Alaskan coastal plain near Point Barrow consisted of grasses, sedges and moss (1.6 km^2 catchment).

Uncertainties in the measured fluxes were assessed for some of these field observations. These uncertainties are: 5%–10% for the energy fluxes near Manaus; within 10 W m^{-2} (about 20%) for the monthly values of net radiation and latent heat flux near Cabauw; about 10% and 12%, respectively, for net radiation and evaporation near Janlappa. Tajchman et al. (1997) have noted possible leakage in the catchment near Parsons.

2.2. River basins

A biophysical process-based model driven by surface and satellite measurements (Choudhury and DiGirolamo, 1998, http://hydro4.gsfc.nasa.gov) was used to calculate evaporation from ten river basins (Amazon, Changjiang, Congo, Mississippi, Nile, Ob, Parana, St. Lawrence, Volga and Yenisey) for four years (1987–1990). Total evaporation is obtained by calculating interception according to Horton (1919), transpiration from the Penman–Monteith equation (Monteith, 1981) with minimum canopy stomatal resistance determined from the rate of carbon assimilation, and soil evaporation according to either energy limited or exfiltration limited rate (Ritchie, 1972). Snow evaporation occurs at a constant rate for the duration of snowcover. Satellite observations were used to obtain fractional vegetation cover, solar and photosynthetically active radiation, surface albedo, fractional cloud cover, air temperature, and vapor pressure. The friction velocity and surface air pressure were obtained from a four dimensional data assimilation procedure, while precipitation was derived by combining gauge and satellite measurements. A land use and land cover data base (Matthews, 1983) was used to describe geographical distribution of biophysical parameters of the model. All calculations were done at a daily time step and at

Table 3
Comparison of mean annual evaporation (mm) calculated using the biophysical model (Present) with estimates based on the atmospheric water budget analysis (Budget) for five river basins. Sources of these estimates and absolute difference (%) in the evaporation values are given

Basin	Present	Budget	Difference (%)	Source
Amazon	1038	1139	10	Matsuyama, (1992)
Mississippi	589	621	5	Roads et al., (1994)
Ob	393	288	27	Kuznetsova, (1990)
Parana	951	963	1	Kuznetsova, (1990)
Volga	474	481	2	Kuznetsova, (1990)
All Basins	689	698	1	

$0.25^\circ \times 0.25^\circ$ spatial resolution. Comparisons of calculated evaporation with micrometeorologic measurements at two locations, evaporation estimated using the atmospheric water budget method for two river basins, and the water balance of 132 catchments having different vegetation covers distributed throughout the world gave an uncertainty in the calculated annual evaporation of about 15%. The calculated temporal variation of soil moisture was also in good agreement with observations. Thus, predictions of the model were fairly well tested against observations to provide reasonable confidence in the results.

The calculated means and ranges of annual evaporation (1987–1990) for the river basins are given in Table 2. The annual mean evaporation differs from climatologic values determined by Korzun (1978) by 1%–16% for individual basins, while the average for all basins differ by 2% (Table 2). The mean absolute error (MAE) with respect to Korzun's values is 52 mm, which is 8% of the average evaporation from all basins. The rather large difference for the Nile basin (16%) could be because of the prolonged drought (since early 1970) and land degradation over the Sahel and Sudan zones of Africa (Le Houerou, 1989, p. 85) through which the river passes. Thus,-Korzun (1978, p. 302) gives precipitation over the Nile basin as 730 mm, while it is 647 mm (1987–1990 average) in the present calculations. The ratio of evaporation to precipitation is 0.85 according to Korzun, while it is 0.81 in the present study. However, in comparison with Korzun, we recognize that the present calculations for the four years may not provide climatologic values.

We could not find any other single source where evaporation values for all ten basins are given. However, comparison with evaporation values determined by the atmospheric water budget analysis for five of these basins given in Table 3 show agreement similar to that in Table 2. The rather large difference for the Ob basin is essentially because of the estimated zero evaporation during February, and substantial negative evaporation during January and October according to the budget method. The results in Tables 2 and 3 provide further confidence in the evaporation values derived from the biophysical model.

As in Korzun's analysis, measured runoff for these river basins for the four years needs to be adjusted (seepage, drainage area between the last guaging station to the river mouth, etc.) for computing evaporation. These adjustments have not yet been done to allow a direct comparison with the present calculations.

2.3. Effect of spatial variability

An approximate analytical study was done to assess the effect of spatial variations in P and R_n on determining evaporation from Eq. (3). Specifically, we address the question, how is spatially averaged evaporation related to evaporation calculated using spatially averaged P and R_n?

If P and R_n are independent variables, then spatially averaged evaporation ($\langle E \rangle$) will be given by:

$$\langle E \rangle = \int_0^\infty \int_0^\infty \Phi(P, R_n)\, f(P)\, f(R_n)\, \mathrm{d}P\, \mathrm{d}R_n, \qquad (7)$$

where $\Phi(P, R_n)$ denotes the right hand side of Eq. (3) and is considered here to represent the local evaporation for a specific value of α, and $f(P)$ and $f(R_n)$ are probability distribution functions representing spatial variations of P and R_n (these distribution functions need not be identical). It is assumed that α does not

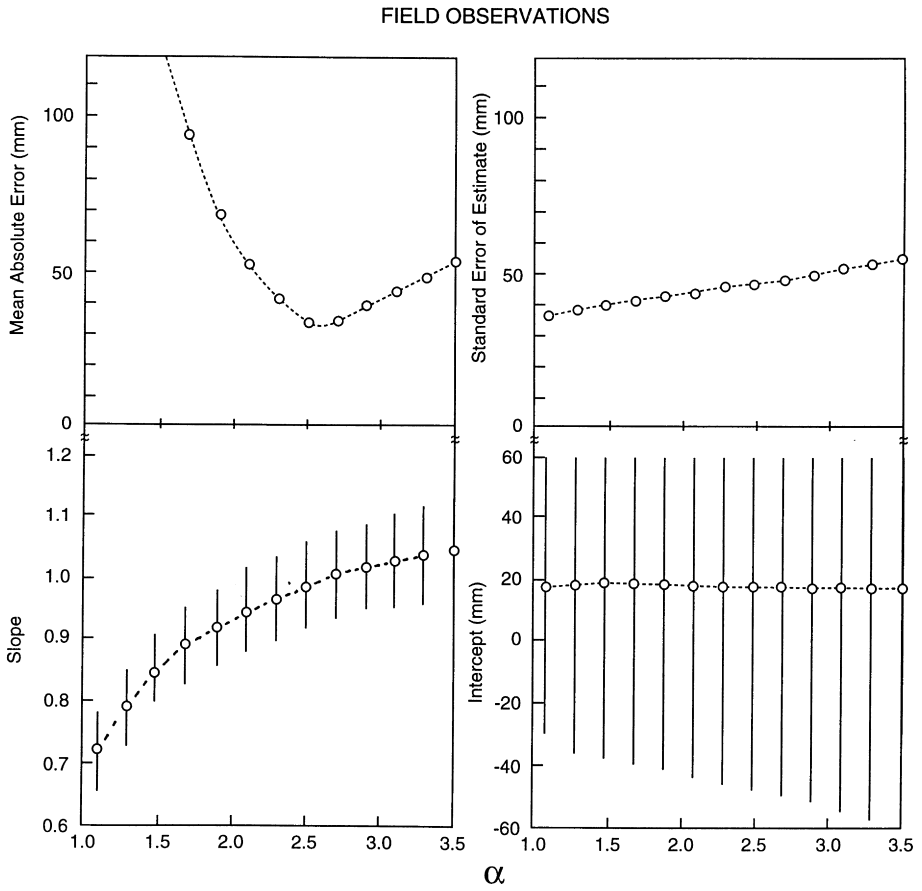

Fig. 1. Variations of the slope and intercept of linear least square regression, standard error of estimate (SEE) and mean absolute error (MAE) with the empirical parameter (α) of Eq. (3) for the data given in Table 1 ($n = 10$). The bars for slope and intercept represent 95% confidence range.

vary spatially, i.e., the model for local evaporation is spatially invariant.

Alternately, if spatially averaged P ($= P_0$) and R_n($= R_{n0}$), defined as:

$$P_0 = \int_0^\infty P\, f(P)\, \mathrm{d}P, \tag{8}$$

$$R_{n0} = \int_0^\infty R_n\, f(R_n)\, \mathrm{d}R_n, \tag{9}$$

are used in Eq. (3), the resulting evaporation will be,

$$\langle E\rangle' = \Phi(P_0, R_{n0}), \tag{10}$$

Our objective is to find the relationship between $\langle E\rangle$ and $\langle E\rangle'$.

By the Taylor series expansion of Φ (P,R_n) in Eq. (7) about $P = P_0$ and $R_n = R_{n0}$ up to the second order term, one can write $\langle E\rangle$ as:

$$\langle E\rangle = \langle E\rangle' + \frac{1}{2}[\Phi''_{P_0}(P_0, R_{n0})\, \sigma^2(P_0) + \Phi''_{R_{n0}}(P_0, R_{n0})\, \sigma^2(R_{n0})], \tag{11}$$

where $\Phi''_{P_0}(P_0, R_{n0})$ and $\Phi''_{R_{n0}}(P_0, R_{n0})$ are the second derivatives of the right hand side of Eq. (3) with respect to P and R_n being evaluated at P_0 and R_{n0}, given by:

$$\Phi''_{P_0}(P_0, R_{n0}) = -(1+\alpha)(\mu)^\alpha/[P_0\{1+(\mu)^\alpha\}], \tag{12}$$

$$\Phi''_{Rn0}(P_0, R_{n0}) = -(1+\alpha)(\mu)/[P_0\{1+(\mu)^\alpha\}], \tag{13}$$

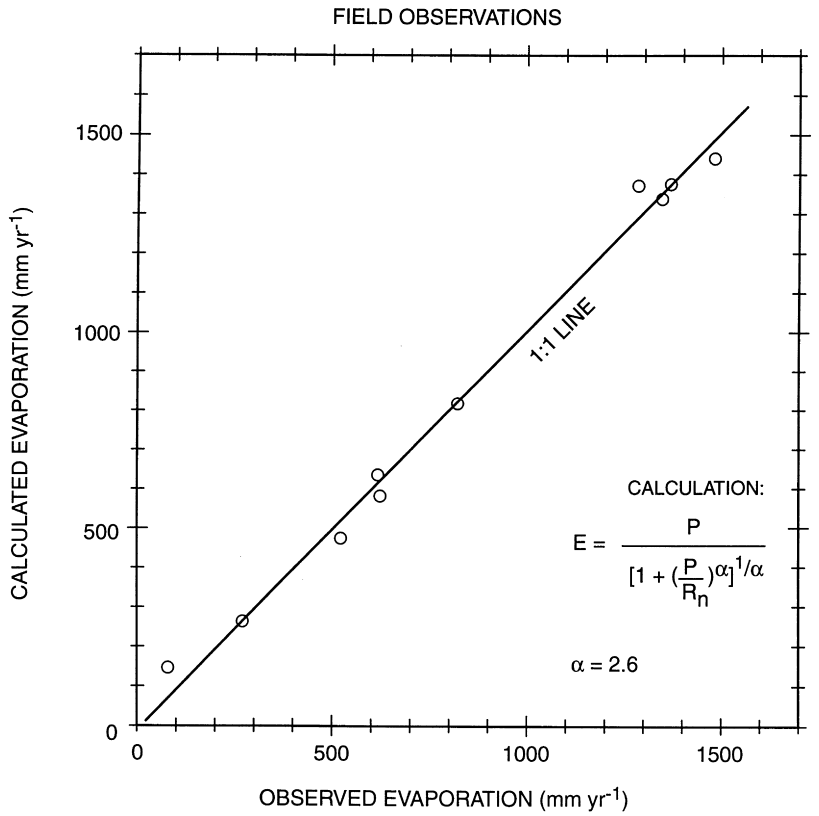

Fig. 2. Scatterplot of the observed and calculated evaporation for $\alpha = 2.6$ for the locations in Table 1.

where $\mu = P_0/R_{n0}$, and $\sigma^2(P_0)$ and $\sigma^2(R_{n0})$ are variances of P and R_n, given by:

$$\sigma^2(P_0) = \int_0^\infty (P - P_0)^2 f(P)\, dP, \tag{14}$$

$$\sigma^2(R_{n0}) = \int_0^\infty (R_n - R_{n0})^2 f(R_n)\, dR_n,$$

As the variances are not negative, while the second derivatives are negative, Eq. (11) shows that $\langle E\rangle$ will be less than $\langle E\rangle'$. Also, differences between $\langle E\rangle$ and $\langle E\rangle'$ will decrease as spatial variability over a catchment decreases (i.e., the distribution functions become strongly peaked around P_0, and R_{n0}).

One can verify that for a given P and R_n, E calculated from Eq. (3) decreases as α decreases (see Section 1). Thus, if spatially averaged values of P and R_n are to be used in Eq. (3), a value of α lower than that providing local evaporation may provide spatially averaged evaporation. As the variances tend to increase with an increase in the spatial scale (Lebel and Le Barbe, 1997), our hypothesis is that the value of α appropriate for the river basins would be lower than that for the field observations. We recognize that factors other than spatial scale can affect the variances.

Some specific results derived from Eq. (7) are given in the Appendix, which attempt to provide a rational basis to the empirical equation.

2.4. Evaluation of the empirical equation

Considering α as an adjustable parameter for fitting the observations, we calculated E from Eq. (3) for each pair of P and R_n in Table 1 for prescribed values of α, and these calculated values were objectively

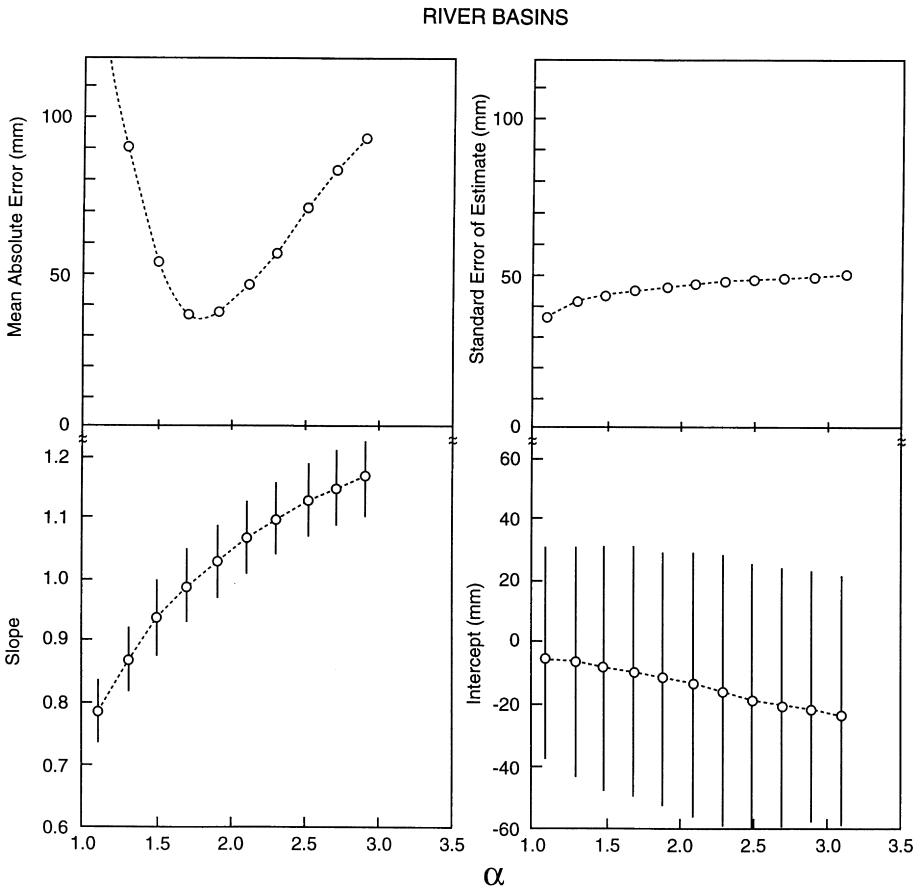

Fig. 3. Variations of the slope and intercept of linear least square regression, SEE and MAE with the empirical parameter (α) for evaporation from 10 river basins for 4 years ($n = 40$). The bars denote 95% confidence range.

evaluated against the correspondingly observed E. Following Willmott (1982), these objective measures were, the explained variance (r^2), slope and intercept of least square linear regression and their 95% confidence limits (for testing the hypothesis that the slope does not differ from 1 and the intercept does not differ from zero), standard error of estimate (SEE), MAE, and index of agreement (d). These measures were also determined for the river basins.

3. Results and discussion

For the field observations, the slope, intercept, SEE and MAE for different values of α are shown in Fig. 1. The intercept did not differ from 0 at 95% confidence level, while the SEE slowly, but steadily increased from 38 to 52 mm with increasing α. The MAE gave minimum value of about 33 mm for values of α in the range 2.5–2.7, and in this range of α values the slope did not differ from 1 at 95% confidence limit. The r^2 and d showed little variation in the range of α values 1.9–3.3 (results not shown); r^2 was in the range 0.991–0.993, while d was in the range 0.992–0.998. Fig. 2 shows the scatterplot of the observed and calculated evaporation for $\alpha = 2.6$. The empirical equation highly overestimates evaporation for the tundra location (the observed and calculated evaporation being, respectively, 72 and 137 mm); the observed and calculated evaporation for each of the other locations differ by less than 8%.

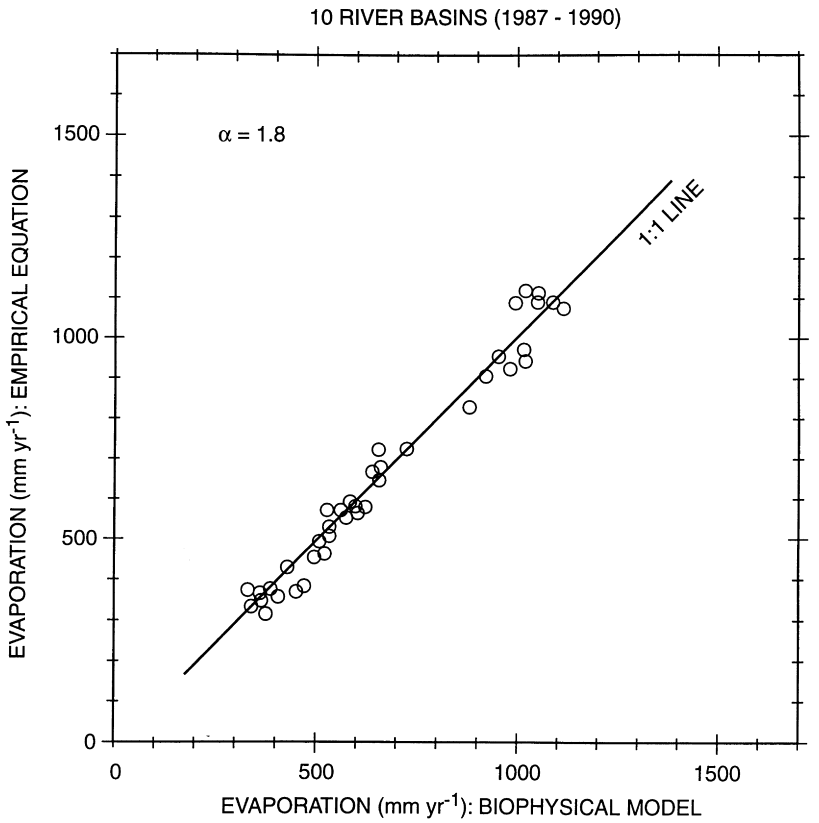

Fig. 4. Scatterplot of evaporation from 10 river basins for 4 years calculated from a biophysical model (Table 2) and from the empirical equation (Eq. (3)) for $\alpha = 1.8$.

For the river basins, variations of the slope, intercept, SEE and MAE with α are shown in Fig. 3. The intercept did not differ from 0 at 95% confidence level, while the SEE slowly, but steadily increased from 38 to 50 mm with increasing α. The minimum value of MAE (about 36 mm) was obtained for $\alpha =$ 1.8, and for this value of α, the slope did not differ from 1 at 95% confidence limit. (The slope does not differ from 1 at 95% confidence limit for values of α in the range 1.7–1.9, although the MAE is little higher, 38 mm). The r^2 showed little variation in the range of α values 1.3–2.3 (r^2 was 0.967–0.972), while d varied from 0.952 to 0.981, achieving a maximum value of 0.992 for $\alpha = 1.8$ (results not shown). Fig. 4 shows the scatterplot of evaporation values calculated from the biophysical model and the empirical equation for $\alpha = 1.8$. Systematic positive and negative differences for all four years were found for five of the basins; the evaporation values calculated from the empirical equation were higher than those from the biophysical model for the Parana and Volga, while they were lower for the Amazon, Changjiang and Nile. The differences for six out of the 40 evaporation values exceeded 10% (these six values were: two each for the Ob and Volga, and one each for the Nile and Yenisey).

These results show that Eq. (3) is fairly effective in explaining variation of E with P and R_n in most cases. These results also show that values of α in the range 2.5–2.7 would apply to the field observations, while the range 1.7–1.9 would be more appropriate for the river basins. That the values of α are lower for the river basins is consistent with our hypothesis (Section 2.3) that variation of E with P and R_n, as determined by α, could change with spatial scale.

If we assume R_n to be synonymous with E_0, then, as

noted in Section 1, Eq. (3) for $\alpha = 2$ gives results which are very close (within ca. 3%) to those given by Eq. (1). It is interesting to note that this value of α (= 2) is within the values found here for field observations (2.6) and large river basins (1.8). For $\alpha = 2$, the MAE for field observations and large river basins would be, respectively, 58 and 41 mm (which are, respectively, 7% and 6% of the mean evaporation), as compared to the optimized MAE of, respectively, 32 and 36 mm. Indeed, if one takes $\alpha = 2$, then, from Eq. (6), the maximum departure in evaporation for some other value of α ($= \alpha'$) close to 2 can be calculated to be, $E(\alpha')/E(2) = 1 + (\alpha' - 2)(\ln 2)/4$, and thus errors larger than 10% may not occur for many catchments when $\alpha = 2$ is assumed. The regression slope, however, differs from 1 at 95% confidence level for field observations, but marginally so for the river basins (Figs. 1 and 3).

4. Summary and conclusions

An empirical equation for annual evaporation based on precipitation and net radiation, and an adjustable parameter was evaluated using field measurements (micrometeorologic and water balance data for small catchments), and results from a biophysical process-based model for four years (1987–1990) for ten large river basins. While the equation was found to be fairly effective in explaining the evaporation values (the MAE was about 5%, and the explained variance was about 98%), the optimized values of the parameter were found to be different for field measurements and the river basins. An approximate analytical study suggested that spatial variabilities in precipitation and net radiation could affect the value of the empirical parameter. The equation highly overestimate evaporation from a tundra catchment.

Accuracy and general applicability of the empirical equation will become better clarified as pertinent measurements for annual periods become available at other locations. This stipulation is made because factors determining the value of α are not yet fully understood and no physical explanation is apparent for the large discrepancy found for a tundra catchment. Much effort is being made to derive precipitation and net radiation globally using surface and space-borne measurements, which might be used to estimate annual evaporation and assess its interannual variability, complementing estimates based on physically-based models.

Acknowledgements

Data processing assistance was provided by Nick DiGirolamo. Prof. T. Oki provided digital templates for the boundaries of the river basins.

Appendix

This appendix provides some specific results derived from Eq. (7) considering models of local evaporation and spatial variations of precipitation and net radiation.

If evaporation at any point is taken to be equal to the minimum of precipitation and net radiation at that location, which is the limiting case of $\Phi(P,R_n)$ in Eq. (7) when α tends to infinity (this will logically be a limit to consider if α is assumed to increase with decreasing spatial scale), then spatially averaged evaporation ($\langle E \rangle$) would be given by:

$$\langle E \rangle = \int_0^\infty \int_0^\infty \min(P, R_n)\, f(P)\, f(R_n)\, dP\, dR_n, \qquad (A.1)$$

which can be written explicitly as:

$$\langle E \rangle = \int_0^\infty f(R_n)\, dR_n \int_0^{R_n} P\, f(P)\, dP + \int_0^\infty R_n\, f(R_n)\, dR_n \int_{R_n}^\infty f(P)\, dP. \qquad (A.2)$$

Now, assuming the distribution function for precipitation to be exponential, i.e.,

$$f(P) = P_0^{-1} \exp(-P/P_0), \qquad (A.3)$$

while the distribution function for net radiation to be either exponential,

$$f(R_n) = R_{n0}^{-1} \exp(-R_n/R_{n0}), \qquad (A.4a)$$

or uniform,

$$f(R_n) = \delta(R_n - R_{n0}), \qquad (A.4b)$$

where P_0 and R_{n0} are spatially averaged values (Eqs. (8) and (9)) and $\delta(R_n - R_{n0})$ is Dirac's delta function, the integrals in Eq. (A.2) can be evaluated to give $\langle E \rangle$

for exponential distribution of net radiation (Eq. (A.4a)) as:

$$\langle E\rangle = P_0/(1+\mu), \tag{A.5a}$$

where $\mu = P_0/R_{n0}$, and for uniform distribution of net radiation (Eq. (A.4b)) as:

$$\langle E\rangle = P_0\{1-\exp(-1/\mu)\}, \tag{A.5b}$$

One can recognize Eq. (A.5a) to be a special case of Eq. (3) when $\alpha = 1$, while Eq. (A.5b) is the Schreiber (1904) equation (the first bracketed term in Eq. (1)) when potential evaporation (E_0) considered to be synonymous with net radiation. As Eq. (A.5a) is obtained using distributions of P and R_n which are weighted at the low end of their values, this equation might be considered to provide a lower limit for $\langle E\rangle$, and, in this respect, Eq. (A.5b) would be a more reasonable lower limit because net radiation has not been similary weighted. Previous studies had concluded that Schreiber's equation generally underestimates evaporation.

If one assumes a gamma distribution for P, i.e.,

$$f(P) = P^{(a-1)}(a/P_0)^a \exp(-aP/P_0)/\Gamma(a), \tag{A.6}$$

(where a is an adjustable parameter and $\Gamma(a)$ is the gamma function) and an uniform distribution for R_n (Eq. A.4b), the resulting equation for $\langle E\rangle$ would be,

$$\langle E\rangle = P_0[\gamma(a+1, a/\mu)/a + (1/\mu)\Gamma(a, a/\mu)]/\Gamma(a), \tag{A.7}$$

where $\gamma(x,y)$ and $\Gamma(x,y)$ are incomplete gamma functions.

Eq. (A.7) can be expressed in terms of elementary functions for integer values of a. Thus, while Eq. (A.5b) is obtained for $a = 1$, for $a = 2$ one obtains,

$$\langle E\rangle = P_0[1-\{(1+\mu)/\mu\}\exp(-2/\mu)]. \tag{A.8}$$

Evaporation values predicted by Eq. (A.8) are within 6% of those predicted by Eq. (3) for $\alpha = 2$. A similar analytic expression for $\langle E\rangle$ can be written for $a = 3$, which gives results within 6% of those predicted by Ol'dekop (1911) equation (the second bracketed term in Eq. (1)). Thus, while Eq. (A.7) does not exactly match the predictions of the empirical equations, it does provides a rational basis for understanding the general pattern of these predictions.

References

Beljaars, A.C.M., Bosveld, F.C., 1997. Cabauw data for the validation of land surface parameterization schemes. J. Clim. 10, 1172–1193.

Bovis, M.J., Barry, R.G., 1974. A climatologic analysis of north polar desert areas. In: Smily, T.L., Zumberge, J.H. (Eds.). Polar Deserts and Modern Man, University of Arizona Press, Tucson, pp. 23–31.

Brown, J., Dingman, S.L., Lewellen, R.I., 1968. Hydrology of a drainage basin on the Alaskan coastal plain, Research Report 240, U.S. Army Cold Region Research and Engineering Laboraroty. Hanover, New Hampshire, pp. 18.

Brutsaert, W., 1982. Evaporation into the Atmosphere. Reidel, Boston.

Budyko, M.I., 1958. The Heat Balance of the Earth's Surface. U.S. Department of Commerce. Washington, D.C.

Calder, I.R., Wright, I.R., Murdiyarso, D., 1986. A study of evaporation from tropical rain forest – west Java. J. Hydrol. 89, 13–31.

Choudhury, B.J., DiGirolamo, N.E., 1998. A biophysical process-based estimate of global land surface evaporation using satellite and ancillary data. I. Model description and comparison with observations. J. Hydrol. 205, 164–185.

Dooge, J.C.I., 1992. Sensitivity of runoff to climate change: A Hortonian approach. Bull. Am. Meteorol. Soc. 73, 2013–2024.

Foley, J.A., Prentice, I.C., Ramankutty, N., Levis, S., Pollard, D., Sitch, S., Haxletine, A., 1996. An integrated biosphere model of land surface processes, terrestrial carbon balance, and vegetation dynamics. Global Biogeochem. Cycle 10, 603–628.

Holscher, D., Sa, T.D. de A., Bostos, T.X., Denich, M., Folster, H., 1997. Evaporation from secondary vegetation in eastern Amazonia. J. Hydrol. 193, 293–305.

Horton, R.E., 1919. Rainfall interception. Mon. Wea. Rev. 47, 603–623.

Jaeger, L., Kessler, A., 1997. Twenty years of heat and water balance climatology at the Hartheim pine forest. Germany. Agric. For. Meteorol. 84, 25–36.

Korzun, V.I. (Ed.), 1978. World Water Balance and Water Resources of the Earth. UNESCO, Paris.

Kuznetsova, L.P., 1990. Use of data on atmospheric moisture transport over continents and large river basins for the estimation of water balances and other purposes. UNESCO, Paris.

Lebel, T., Le Barbe, L., 1997. Rainfall monitoring during HAPEX-Sahel. 2. Point and areal estimation at the event and seasonal scales. J. Hydrol. 188/189, 97–122.

Le Houerou, H.N., 1989. The Grazing Land Ecosystems of the African Sahel. Springer-Verlag, New York.

Liang, G., 1982. Net radiation, potential and actual evapotranspiration in Austria. Arch. Meteorol. Geophys. Bioklim. B31, 379–390.

Lieth, H., 1975. Modeling the primary productivity of the world. In: Lieth, H., Whittaker, R.H. (Eds.). Primary Productivity of the Biosphere, Springer-Verlag, New York, pp. 237–263.

L'vovich, M.I., 1979. World Water Resources and their Future. American Geophysical Union, Washington, DC.

Matsuyama, H., 1992. The water budget in the Amazon river basin

during the FGGE period. J. Meteorol. Soc. Japan 70, 1071–1083.
Matthews, E., 1983. Global vegetation and land use: new high resolution data bases for climate studies. J. Clim. Appl. Meteorol. 22, 474–487.
Maykut, G.A., Church, P.E., 1973. Radiation climate of Barrow, 1962–1966. J. Appl. Meteorol. 12, 620–628.
Monteith, J.L., 1981. Evaporation and surface temperature. Q. J. R. Meteorol. Soc. 107, 1–27.
Ol'dekop, E.M., 1911. On evaporation from the surface of river basins. Trans. Meteorol. Observ. University of Tartu, 4, pp. 200 and 20 figures.
Packer, R.W., Sangal, B.P., 1971. The heat and water balance of southern Ontario according to the Budyko method. Can. Geograph. 15, 262–286.
Penman, H.L., 1948. Natural evaporation from open water, bare soil and grass. Proc. R. Soc. Lond. A 193, 120–148.
Pike, J.G., 1964. The estimation of annual run-off from meteorological data in a tropical climate. J. Hydrol. 2, 116–123.
Ritchie, J.T., 1972. Model for predicting evaporation from a row crop with incomplete cover. Water Resour. Res. 8, 1204–1213.
Roads, J.O., Chem, S.-C., Guetter, A.K., Georgakakos, K.P., 1994. Large-scale aspects of United States hydrologic cycle. Bull. Am. Meteorol. Soc. 75, 1589–1610.
Ryden, B.E., 1981. Hydrology of northern Tundra. In: Bliss, L.C., Heal, O.W., Moore, J.J. (Eds.). Tundra Ecosystems: A Comparative Analysis, Cambridge University Press, New York, pp. 115.
Schreiber, P., 1904. Uber die Beziehungen zwischen dem Niederchlag und der Wasserfuhrung der Flusse in Mittelleuropa. Z. Meteorol. 21, 441–452.
Shuttleworth, W.J., 1988. Evaporation from Amazonian rainforest. Proc. R. Soc. Lond. B 233, 321–346.
Tajchman, S.J., Fu, H., Kochenderfer, J.N., 1997. Water and energy balance of a forested Appalachian watershed. Agr. For. Meteorol. 84, 61–68.
Turc, L., 1954. Le bilan d'eau des sols: relations entre les precipitations l'evaporation el l'ecoulement. Ann. Agron. 5, 491–595.
Unland, H.E., Houser, P.R., Shuttleworth, W.J., Yang, Z.-L., 1996. Surface flux measurement and modeling at a semi-arid Sonaran Desert site. Agric. For. Meteorol. 82, 119–153.
Vogt, R., Jaeger, L., 1990. Evaporation from a pine forest-using the aerodynamic method and Bowen ratio method. Agric. For. Meteorol. 50, 39–54.
Willmott, C.J., 1982. Some comments on the evaluation of model performance. Bull. Am. Met. Soc. 63, 1309–1313.
Zubenok, L.I., 1976. Evaporation from continents. Main Geophysical Observatory, Gidrometeoizdat, Leningrad.